

Interannual Variations of the Intraseasonal Oscillation in the South Asian Summer Monsoon Region

DAVID M. LAWRENCE AND PETER J. WEBSTER

Program in Atmospheric and Oceanic Sciences, University of Colorado, Boulder, Colorado.

(Manuscript received 24 February 2000, in final form 29 November 2000)

ABSTRACT

It is noted that the behavior of the intraseasonal oscillation (ISO) of the south Asian monsoon varies from year to year. An index representing seasonally averaged ISO activity is developed using outgoing longwave radiation data for the period 1975–97. Interannual variations in ISO activity are found to be related to year-to-year changes in the number of discrete events rather than to changes in the characteristic period.

Summertime ISO activity exhibits a reasonably strong inverse relationship with Indian monsoon strength but not with total south Asian monsoon strength primarily because of a lack of correlation between ISO activity and the Bay of Bengal component of the south Asian monsoon. Over the 22-yr period examined here, the relationship between Indian monsoon strength and ISO activity is comparable to or even stronger than the well-documented relationship with El Niño–Southern Oscillation (ENSO). However, summertime ISO activity is found to be relatively uncorrelated with ENSO except for a weakly positive correlation at the beginning of the south Asian monsoon season. Therefore, the ISO activity–Indian monsoon relationship is essentially independent of the ENSO–Indian monsoon relationship. ISO activity is uncorrelated with any other contemporaneous or leading sea surface temperature variability.

1. Introduction

The interannual variability of the south Asian monsoon has been the subject of extensive research [for review, see Webster et al. (1998)], particularly because of the profound social and economic consequences for the large agrarian populations of south Asia and also because of the monsoon's influence on global circulation. Consequently, seasonal prediction of the monsoon has long been a goal of forecasters. Statistical forecasts have been moderately successful (Krishna Kumar et al. 1995), but accurate dynamical seasonal prediction has thus far proven elusive (Brankovic and Palmer 2000).

In part, the difficulties encountered with dynamic seasonal prediction of the monsoon are caused by the complex and diverse forcings that impact seasonal monsoon strength. These forcings include the extensively studied inverse relationship with the El Niño–Southern Oscillation (ENSO; Yasunari 1990; Webster and Yang 1992; Webster 1995; Ju and Slingo 1995; Wainer and Webster 1996), which is complicated by interdecadal changes in the robustness of the relationship (Elliot and Angell 1988; Torrence and Webster 1999). Indian Ocean SST anomalies may also play a role (e.g., average March–

May Arabian Sea SST, Rao and Goswami 1988; preceding fall and winter Indian Ocean SST, Harzallah and Sadoury 1997; Clark et al. 2000). A biennial oscillation in monsoon rainfall is also a factor (Mooley and Parthasarathy 1984) and may be related to the tropospheric biennial oscillation that is found in many atmospheric variables including precipitation, surface pressure, tropospheric winds, and SST (Meehl 1987, 1997) or to biennial variations in Eurasian snow cover (Vernekar et al. 1995; Yang 1996).

Another potential source of interannual fluctuations in south Asian monsoon strength is interannual changes in intraseasonal variability (Sperber et al. 2000). A dominant characteristic of intraseasonal fluctuations during summer in the monsoon region is the active–break cycles of precipitation over south Asia that exhibit periods around 30–60 days (e.g., Yasunari 1979; Sikka and Gadgil 1980; Gadgil and Asha 1992). The active–break cycles are linked to observed northward propagation of convection from the equatorial Indian Ocean (Lau and Chan 1986; Wang and Rui 1990; Gadgil and Asha 1992) that in turn appears to be linked to the eastward movement of convection associated with the intraseasonal or Madden–Julian oscillation (ISO; Julian and Madden 1981; Lau and Chan 1986).

There is some evidence that interannual variations of ISO activity may influence seasonal monsoon strength. Hendon et al. (1999) found that global ISO activity during boreal winter is inversely related to Australian

Corresponding author address: David M. Lawrence, Department of Meteorology/CGAM, University of Reading, Earley Gate, P.O. Box 243, Reading, Berkshire RG1 6BB, United Kingdom.
E-mail: dml@met.rdg.ac.uk

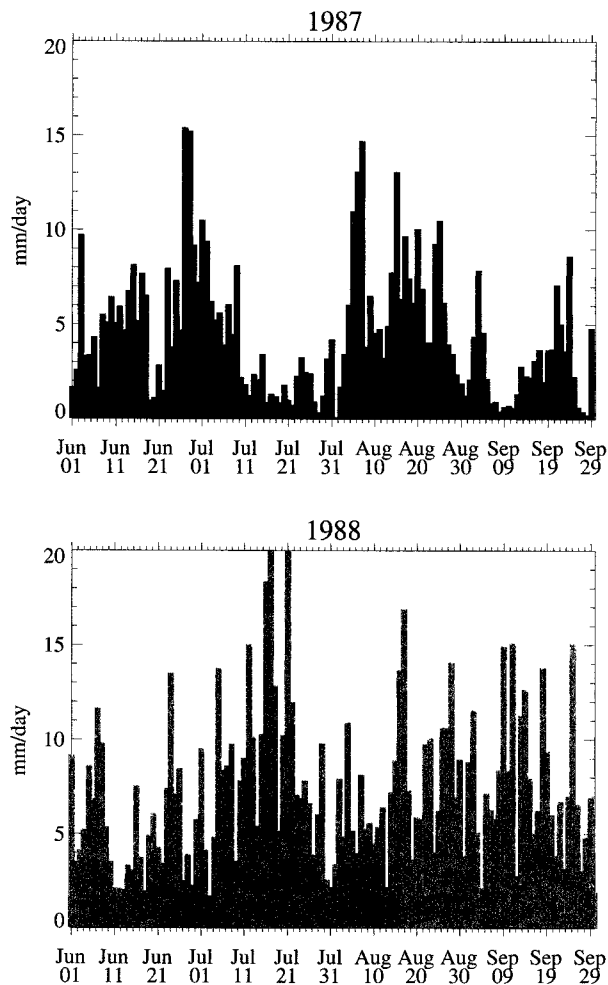


FIG. 1. Time series of daily precipitation rate estimates averaged over 10° – 15° N, 75° – 80° E for Jun–Sep 1987 and 1988 (mm day^{-1}).

monsoon strength. In other words, winter seasons that are characterized by strong and numerous intraseasonal oscillations tend to correspond to seasons of reduced North Australian monsoon rainfall. However, there are significant differences between the winter and summer ISOs and the south Asian and Australian monsoons. For example, the ISO is considerably stronger and more regular during northern winter (e.g., Madden 1986; Hendon and Salby 1994) and the Australian monsoon is located closer to the equator, where the ISO is most influential, than the south Asian monsoon.

A number of authors have observed year-to-year variability in the strength and character of the summertime ISO. Yasunari (1980) observed that the characteristic period of oscillation increased significantly to near 60 days during the summer of 1972, a severe drought year in India, compared to the typical 40-day period. Mehta and Krishnamurti (1988) found that certain summers exhibit regular northward propagation of convection whereas during other summers the northward propagation is irregular or absent entirely. Singh et al. (1992)

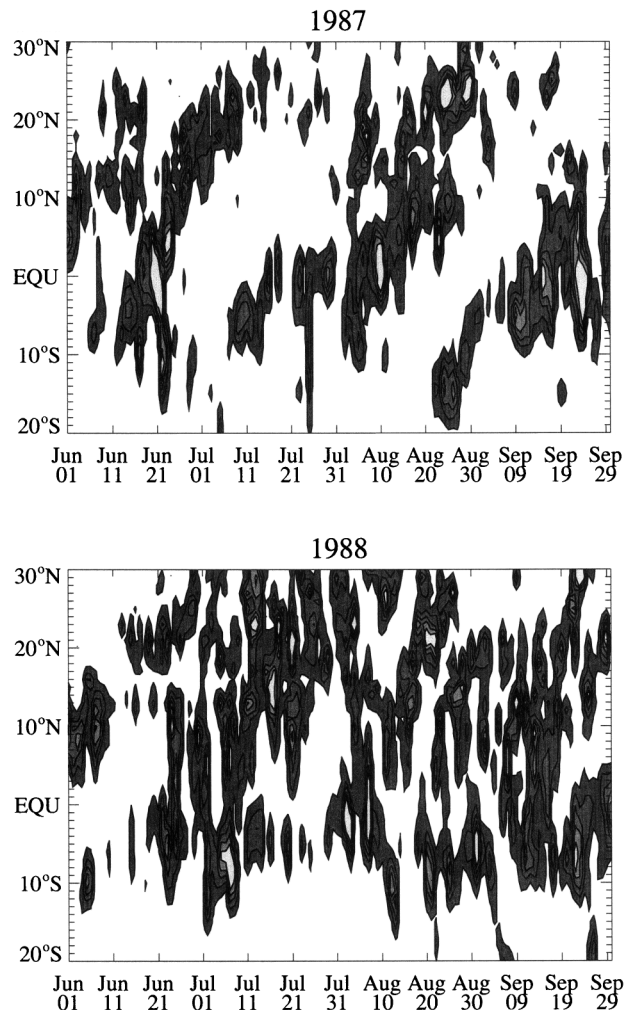


FIG. 2. Time–latitude section of daily precipitation rate estimates along 75° – 80° E for Jun–Sep 1987 and 1988. Contour interval is 5 mm day^{-1} with the first contour at 5 mm day^{-1} .

found that the seasonal ISO intensity varies by half to double its average intensity. Chowdhury et al. (1988) showed, from limited data, that the interannual variability of ISO activity is related to the overall monsoon strength. Ferranti et al. (1997), using data from five 10-yr European Centre for Medium-Range Weather Forecasts Atmospheric Model Intercomparison Project integrations, found that intraseasonal and interannual fluctuations have a common dominant mode of variability in the Asian monsoon region.

An example of year-to-year changes in ISO behavior is demonstrated in Fig. 1, which displays daily time series of precipitation over central India for the 1987 and 1988 summers, and Fig. 2, which shows time–latitude sections of precipitation along 75° – 80° E for the same two seasons. The 1987 summer season is marked by three distinct active periods each separated by about 40 days. Comparison with the time–latitude section in Fig. 2 reveals that all three active periods over central

India are associated with northward-propagating systems of precipitation. Conversely, during the 1988 summer season, no well-defined active or break periods are discernible. Instead, the precipitation time series is marked by relatively steady rainfall from one day to the next throughout the season. In particular, the 1988 summer is largely devoid of low rainfall days. Moreover, evidence of coherent northward movement of envelopes of precipitation is largely absent, excepting perhaps an event around 1–21 July. Vernekar et al. (1993) previously noted a marked difference in ISO intensity between 1987, when ISO intensity was high, and 1988, when ISO activity was virtually absent.

For the purposes of prediction, the causes behind interannual changes in ISO activity have been sought. Previous studies of interannual variations of ISO activity have searched for a relationship with ENSO. Hendon et al. (1999) and Slingo et al. (1999) found that the amplitude of wintertime ISO activity is essentially uncorrelated with tropical eastern Pacific SST anomalies or any other SST anomalies for that matter. However, there does appear to be a detectable eastward displacement of wintertime ISO activity during a warm ENSO event (Gutzler 1991; Fink and Speth 1997; Hendon et al. 1999). The relationship between ENSO and summertime ISO activity is not as well understood, but, through experiments with a 5-level global spectral model, Krishnan and Kasture (1996) found that the northward propagation of convection is more regular, and of slower period, for warm ENSO experiments.

The purpose of this paper is to investigate the relationship between interannual variations of ISO activity and south Asian monsoon strength. The role of boundary forcings on summertime ISO activity will also be examined.

This study begins with a description of the datasets used to evaluate ISO activity, monsoon strength, and ENSO (section 2). Section 3 introduces the monsoon strength indices that are used and briefly examines the monsoon–ENSO relationship according to these indices. An objective measure of summertime ISO activity is defined in section 4. The ISO activity index is subsequently used in section 5 to explore the relationships between summertime ISO activity, ENSO, and the south Asian monsoon. Section 6 is devoted to a summary and discussion.

2. Data

The interannual variability of the ISO in the south Asian monsoon region is assessed here with outgoing longwave radiation (OLR) data (Liebmann and Smith 1996). The remotely sensed OLR data are regularly utilized as a proxy for deep tropical convection and consequently as a means of investigating ISO convection. The OLR data are available on a global 2.5° grid from June 1974 to December 1997, except for a 10-month

gap in 1978. This study analyzes data from 22 boreal summers, 1975–97, excluding 1978.

OLR and the all-India rainfall index (AIRI) are used to evaluate monsoon strength (indices defined in next section). The all-India rainfall index is a weighted average of 306 well-distributed rain gauge stations across India (Parthasarathy et al. 1992, 1994), averaged across the June–September period, and is available for the entire period considered in this study.

The state of ENSO is evaluated here using the Niño-3 SST index, which is calculated by averaging monthly Reynolds SST over the domain 5°S – 5°N , 150° – 90°W . Prior to 1982, monthly SST estimates are derived from reconstructed monthly mean SST (Smith et al. 1996) that are based on in situ observations and are interpolated with EOFs. In subsequent years, weekly SST analyses are based on an optimum interpolation of in situ and satellite observations (Reynolds and Smith 1994).

A primary limitation of this study is the relatively short record length employed. This limitation is not easily overcome for diagnostic studies of ISO interannual variability as the 22-yr record of OLR is the best and longest dataset available for the purpose of evaluating ISO activity. Theoretically, the 40-yr National Centers for Environmental Prediction–National Center of Atmospheric Research (NCEP–NCAR) reanalysis dataset could also be used to examine interannual changes in ISO activity. To this point, however, the quality of the NCEP–NCAR data prior to the common availability of satellite wind information in the late 1970s is unclear. The lack of satellite information is particularly harmful to the reanalysis in data-sparse regions such as the Indian Ocean basin. Consequently, we only use the 22-yr OLR dataset in this study and rely upon significance tests to evaluate our results. Making use of the two-tailed Student's t test, the minimum significant correlation coefficients between two time series with 22 degrees of freedom (dof; one for each season) are 0.28, 0.36, and 0.49 for the 90%, 95%, and 99% confidence levels.

3. Monsoon indices and review of monsoon–ENSO relationship

a. Monsoon indices

The choice of an appropriate index that faithfully represents the south Asian summer monsoon interannual variability has been a contentious issue in recent years (Webster and Yang 1992; Goswami et al. 1999; Wang and Fan 1999). A myriad of dynamic and convective indices have been derived each of which containing its own merits and applications. Much of the controversy has revolved around the definition of an appropriate dynamical index. Since we are interested primarily in the interannual variability of rainfall in the south Asian monsoon region and its relationship to interannual changes in ISO activity we will avoid the more contro-

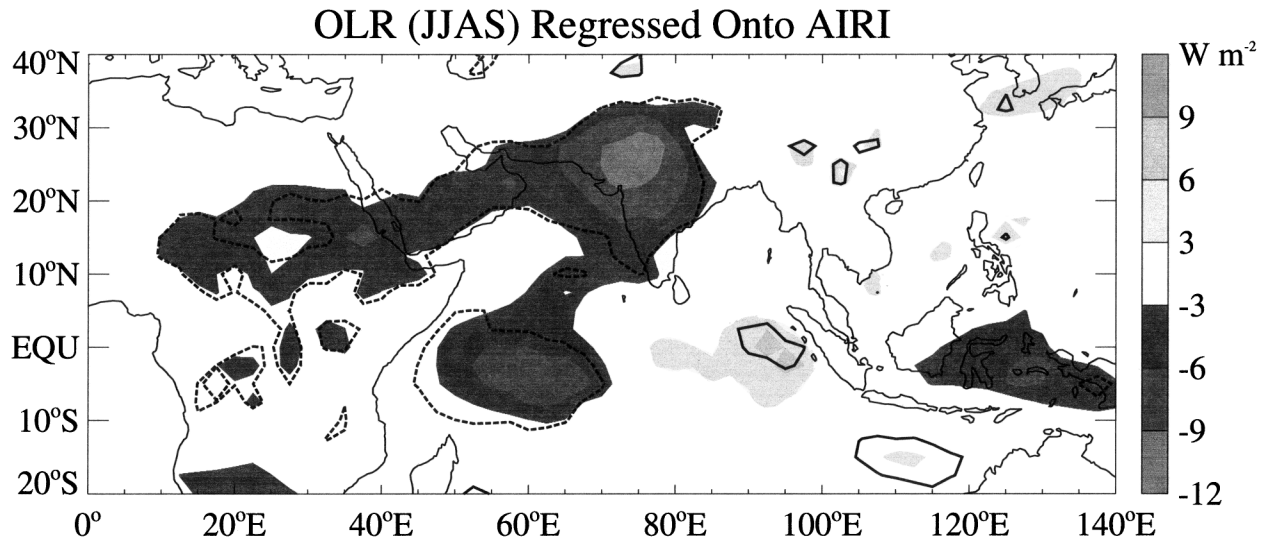


FIG. 3. Regression of Jun–Sep mean OLR onto AIRI. Dashed lines indicate where the regression correlation coefficients exceeded the 95% significance level based on 22 dof (± 0.36).

versal dynamic indices and rely upon the somewhat less controversial convective indices.

The AIRI is commonly used to evaluate variability of the Indian monsoon. Goswami et al. (1999) show that the extended Indian monsoon rainfall (EIMR) index, which is the seasonally averaged precipitation (monthly analyses; Xie and Arkin 1996) for both the Indian subcontinent and the Bay of Bengal (10° – 30° N, 70° – 110° E), is a good measure of the total south Asian monsoon rainfall. Wang and Fan (1999) suggest a convective index (CI) that is based on OLR in the region 10° – 25° N, 70° – 100° E that also is meant to reflect the seasonal precipitation in the south Asian monsoon region. Over the period 1979–97, the EIMR and the CI indices correlate reasonably well at approximately -0.75 . Recall that low OLR values correspond to areas of deep convection and precipitation; therefore, a strongly negative correlation between the AIRI and OLR indicates agreement. Here, we use the CI index since the available record is a few years longer than that for the EIMR index.

Figure 3 shows the regression of seasonal mean OLR

at all grid points in the Indian Ocean basin onto the AIRI. High anticorrelations and low regressed OLR values are seen across India and the Arabian Sea and even over portions of East Africa (for discussion on relationship between AIRI and East African rainfall, see Camberlin 1997). However, the relationship between the AIRI and the seasonal mean OLR over the Bay of Bengal is minimal suggesting that precipitation over India varies somewhat independently from precipitation over the Bay of Bengal. While the reasons behind such independent variability is not clear, the regression results, nonetheless, highlight the importance of considering the interannual variability of the two regions both independently and as a unit. Consequently, we will also make use of two regionally based OLR indices, OLR_{IM} (Indian monsoon), which is the seasonal mean OLR averaged only over Indian landmass grid points and OLR_{BB} (Bay of Bengal), which is the seasonal mean OLR averaged only over Bay of Bengal grid points. For the sake of uniformity, we will refer to the CI as OLR_{SAM} (south Asian monsoon).

The interannual relationships between the monsoon indices are summarized in Table 1, which lists the correlations among all the indices. As anticipated by the regression results shown in Fig. 3, the AIRI does not correlate well with OLR_{BB} but does correlate well with OLR_{IM} . The average correlation between OLR_{BB} and OLR_{IM} supports the above observation that these two regions of the south Asian monsoon vary somewhat independently although clearly they are not fully independent.

TABLE 1. Correlations between seasonal mean south Asian monsoon indices over 22 yr (1975–97, excluding 1978). A correlation coefficient greater than ± 0.36 is statistically significant at 95% confidence level.

Monsoon index	AIRI ^a	OLR_{SAM} ^b	OLR_{IM} ^c	OLR_{BB} ^d
AIRI	—			
OLR_{SAM}	-0.40	—		
OLR_{IM}	-0.70	0.85	—	
OLR_{BB}	-0.04	0.83	0.52	—

^a All-India rainfall index.

^b OLR averaged over 10° – 25° N, 70° – 100° E.

^c OLR averaged over Indian subcontinent grid points only.

^d OLR averaged over Bay of Bengal grid points only.

b. Monsoon–ENSO relationship

Over the 22 yr considered in this study, the simultaneous correlations between June–September (JJAS)

TABLE 2. Correlations between Niño-3 SST and south Asian monsoon indices over 22-yr period (1975–97, excluding 1978).

	AIRI	OLR _{SAM}	OLR _{IM}	OLR _{BB}
JJAS Niño-3 SST	-0.32	0.28	0.44	0.02
DJFM Niño-3 SST	-0.43	0.33	0.43	0.04

Niño-3 SST and the AIRI, OLR_{SAM}, OLR_{IM}, and OLR_{BB} are -0.32, 0.18, 0.44, and 0.02, respectively (see Table 2). Correlations are slightly greater if the subsequent DJF Niño-3 SST is used to represent ENSO (the stronger correlations are due to wintertime peak in evolution of ENSO events; Torrence and Webster 1999). Over the entire record dating back to 1871 the correlation between ENSO and the AIRI is -0.65 (Torrence and Webster 1998) although the robustness of the relationship seems to change on decadal timescales (Torrence and Webster 1999). The relatively weak correlations over the 22-yr record considered here may reflect recent observations that the monsoon-ENSO relationship is entering a weak phase (Goswami et al. 1999; Kumar et al. 1999). For example, despite the near-record strength of the 1997 El Niño, the Indian monsoon rainfall was close to normal (Webster and Palmer 1997).

4. Measure of boreal summer ISO activity

Hendon et al. (1999) developed a number of techniques to objectively evaluate and isolate boreal winter ISO activity. The first method is based on an empirical orthogonal function (EOF) analysis of intraseasonally filtered OLR (complete OLR dataset bandpass filtered with a Lanczos filter using 121 weights and retaining periods 25–80 days, OLR_{25–80}). Here, EOFs are calculated using an extended summer period (May–October)

and on a limited domain that encompasses the south Asian monsoon region including the area of maximum summertime tropical Eastern Hemisphere OLR_{25–80} variance (20°S–30°N, 40°–180°E, see Fig. 4). The leading two EOFs, shown in Fig. 5a, are not separable according to the criteria suggested by North et al. (1982) and explain about 16% (8.8% and 7.1%) of the intraseasonal (25–80 day) variance within this domain. The two modes closely resemble the leading two OLR EOFs found by Lau and Chan (1986) for the 1975–82 summers. The maximum correlation between the two principal component time series is 0.66 at a 9–10-day lag (Fig. 5b) indicating an oscillation period of around 36–40 days. Together, the leading two EOFs describe a propagating mode that captures the low-frequency convective signature that is unique to the northern summer ISO (Lau and Chan 1986; Wang and Rui 1990) including northward and eastward movement of convection from the central equatorial Indian Ocean. OLR reconstructed from the leading two EOFs will be referred to as OLR_{EOF}.

A second method of isolating wintertime ISO activity described by Hendon et al. (1999) involves filtering the OLR data with a wavenumber-frequency filter retaining periods between 25 and 80 days and eastward wavenumbers 1–3. This method is also effective during summer since wavenumber-frequency spectral calculations show that OLR variance is concentrated at periods between 25 and 80 days and eastward wavenumbers 1–3 at both equatorial and Indian subcontinent latitudes during the summer season (not shown). A primary advantage of this method is that it has the ability to capture interannual geographic displacements of variance whereas the EOF method does not. However, it was found that the geographic displacement of ISO activity

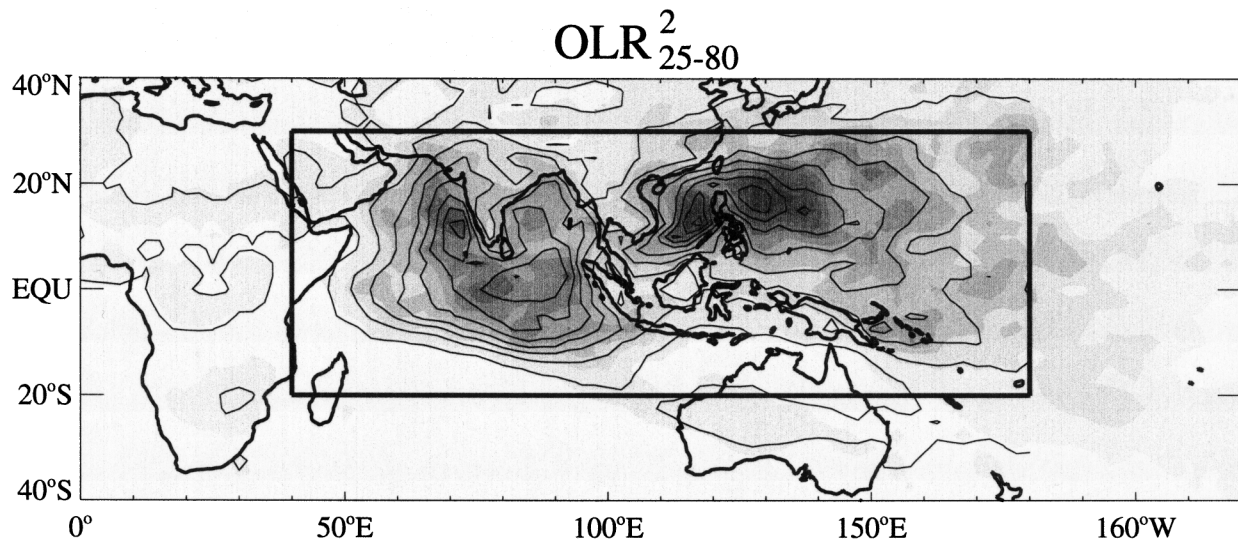


FIG. 4. Climatological variance map for 25–80-day filtered OLR (OLR_{25-80}^2) averaged Jun–Sep 1975–97, excluding 1978. The contour interval is $50 \text{ W}^2 \text{ m}^{-4}$. The interannual standard deviation of variance is shaded with contour intervals of $25 \text{ W}^2 \text{ m}^{-4}$. Box shows domain on which EOF analysis of intraseasonal OLR is completed.

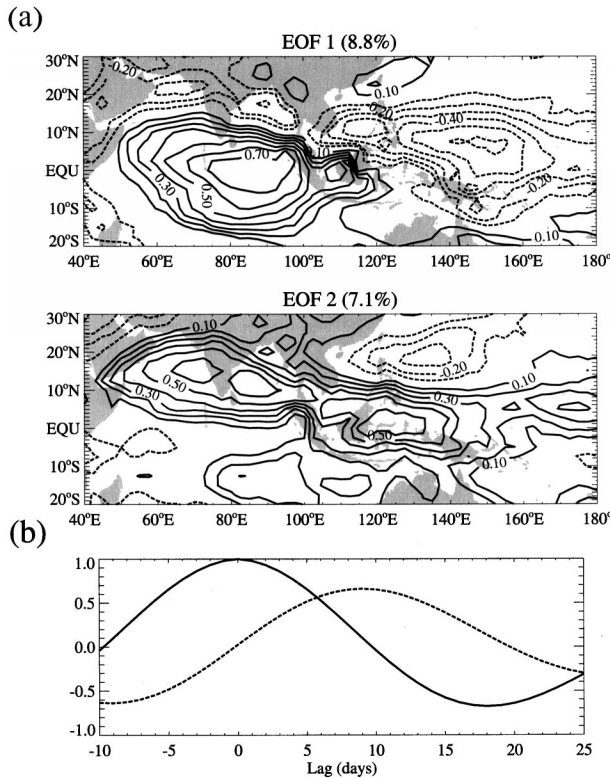


FIG. 5. (a) Leading two EOF loading vectors of extended northern summer 25–80-day filtered OLR. Extended northern summer is May–Oct. EOFs calculated from data in limited domain shown. Contours are every 0.1 with the zero contour omitted. (b) Lagged cross correlation of principal component timeseries. EOF mode 1 with itself (solid line), EOF mode 1 with EOF mode 2 (dashed line).

is minimal from summer to summer and that the ISO activity index derived from wavenumber-frequency filtered data did not differ significantly from the index derived from OLR_{EOF} (interannual correlation between the two indices equals 0.85). Therefore, for the sake of brevity we will present only the results using the EOF method although all the calculations were tested with both ISO activity indices yielding both qualitatively and quantitatively similar results.

To evaluate both the seasonal mean and intraseasonal evolution of ISO activity, the variance of the reconstructed OLR_{EOF} data is assessed using wavelet analysis (for details on wavelet analysis, see Torrence and Compo 1998). At each grid point within the south Asian monsoon region (10°–25°N, 70°–100°E, total of 91 grid points) and for each extended summer season, the wavelet variance spectrum is calculated from 184-day (May–October) OLR_{EOF} time series using a Morlet wavelet basis. The 2002 (91 grid points \times 22 seasons) individual wavelet variance spectra are averaged to produce the composite spectrum shown in Fig. 6.

The composite wavelet variance spectrum (Fig. 6a) exhibits maximum variance in early June at periods just under 40 days. The mean oscillation period slowly in-

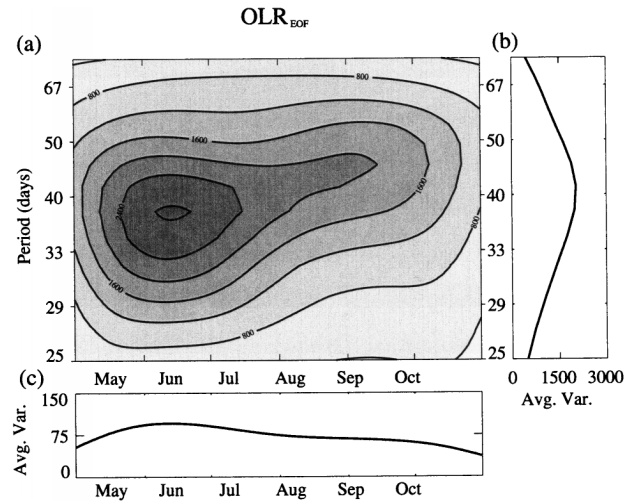


FIG. 6. Wavelet analysis of reconstructed OLR_{EOF} . Wavelet analyses are completed separately on 184-day (May–Oct) OLR_{EOF} time series at each grid point included in 10°–25°N, 70°–100°E. The 91 (7 lat \times 13 long) wavelet spectra are then averaged to generate an areal-averaged wavelet spectrum for each year. The 22 individual wavelet spectra from 1975 to 1997, excluding 1978, are averaged to form an ensemble wavelet variance spectrum. (a) Ensemble average wavelet variance spectrum. Contour levels are every 400 $W^2 m^{-4}$ from white to dark gray. (b) Frequency spectrum generated by averaging (a) over the Jun–Sep period. (c) Variance timeseries generated by scale averaging total variance over 25–80-day period band.

creases from near 37 days at the beginning of the monsoon season to around 46 days by the end of the season. Figure 6b shows the mean frequency spectrum that is generated by averaging the wavelet variance spectrum over the June–September period only. The composite variance time series (Fig. 6c) is derived by computing a weighted average across the individual scales of the total wavelet variance spectrum. The use of wavelet derived variance is chosen in lieu of squared-bandpass variance because, for a wavelet-derived variance estimate, short timescale fluctuations are analyzed with a short window and long timescale fluctuations are analyzed with a long window thus providing a more accurate estimate of the total variance within a period band. The composite variance time series reflects the visible characteristics of the total wavelet spectrum with the highest variance encountered at the beginning of the monsoon season followed by steady mean variance through the rest of the monsoon season before a significant drop in ISO variance during October. The rise in mean ISO variance in May and the fall in mean ISO variance during October reflects the seasonal cycle of the regional influence of the ISO. During the remainder of the year, intraseasonal OLR variance is substantially reduced at Indian subcontinent latitudes as the ISO is located primarily along and to the south of the equator (Madden 1986; Hendon and Salby 1994).

Last, an index that captures the year-to-year variations of summertime ISO activity in the south Asian monsoon region is determined by averaging an individual season's

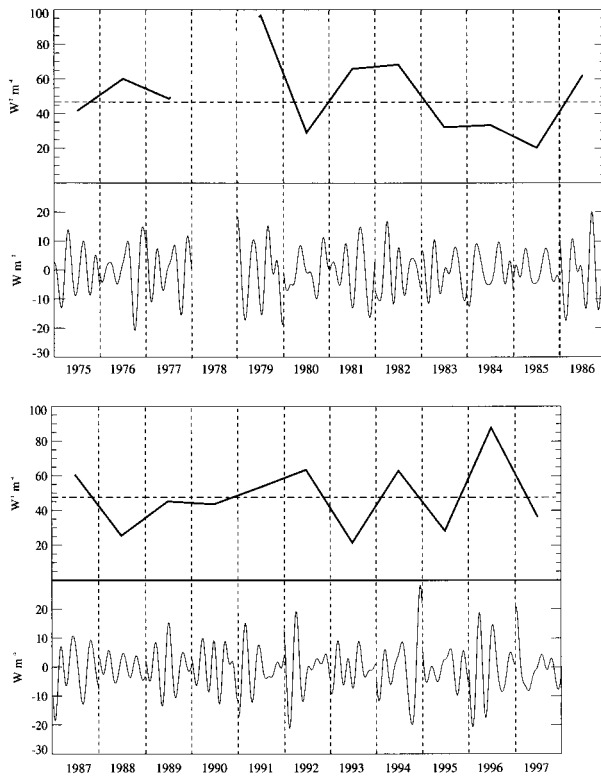


FIG. 7. (top) ISO activity index $[\text{OLR}_{\text{EOF}}^2]$ and (bottom) $[\text{OLR}_{\text{EOF}}]$ time series for JJAS averaged over the core south Asian monsoon region (10° – 25°N , 70° – 100°E). Dashed-dot line indicates mean $[\text{OLR}_{\text{EOF}}^2]$ value.

variance time series (e.g., Fig. 6c except for a single extended summer, not the ensemble mean) across the June–September period. The ISO activity index, $[\text{OLR}_{\text{EOF}}^2]$, is shown in Fig. 7, which also shows the $[\text{OLR}_{\text{EOF}}]$ time series for each summer. Compare, for example, the years 1987 and 1988. As noted in the introduction, 1987 exhibits strong ISO activity that is reflected by its high $[\text{OLR}_{\text{EOF}}^2]$ value ($60 \text{ W}^2 \text{ m}^{-4}$) whereas ISO activity in 1988 is minimal and consequently the associated $[\text{OLR}_{\text{EOF}}^2]$ value is low ($25 \text{ W}^2 \text{ m}^{-4}$).

In the previous section, we found that seasonal mean rainfall over the Indian subcontinent is not strongly correlated to that over the Bay of Bengal. In a similar manner, we split the ISO activity index into a land and an ocean component. Over the 22 seasons examined here, the two components correlate at a level of 0.96, indicating that seasonal changes in ISO activity occur relatively uniformly across the south Asian monsoon region.

5. Interannual variations of ISO activity

a. Changes in ISO characteristics

The magnitude of the ISO activity measure is directly related to the amplitude of the OLR_{EOF} oscillations. Larger-amplitude oscillations lead to more distinct active

and break episodes of rainfall. Active and break episodes can be defined, relative to the central south Asian monsoon region, as minimums and maximums of $[\text{OLR}_{\text{EOF}}]$ that exceed a one standard deviation of $[\text{OLR}_{\text{EOF}}]$. By this definition, the number of discrete active and break events totaled together that occur within each season ranges from one to six. The correlations between $[\text{OLR}_{\text{EOF}}^2]$ and the number of active periods, break periods, and total number active and break periods per season are 0.34, 0.62, and 0.60, respectively.

It is possible to deduce a characteristic ISO period by averaging the seasonal wavelet variance spectrum from June–September (e.g., Fig. 6b except for single season) and identifying the period exhibiting maximum variance. The characteristic periods, determined by this method, vary widely from a low of 27 days to a high of 63 days. The actual spread of ISO periods may not be this broad because, during seasons when the $[\text{OLR}_{\text{EOF}}^2]$ index is low, a characteristic period cannot be distinguished unambiguously due to its weak and nearly flat frequency spectrum (not shown). During seasons when ISO activity is notable (i.e., $[\text{OLR}_{\text{EOF}}^2] > 22\text{-yr}$ mean, see Fig. 7), and therefore a characteristic ISO period can be readily identified, the characteristic period range is limited to between 34 and 45 days.

b. Relation to interannual south Asian monsoon variability

With suitable indices defined for both the seasonal ISO activity and seasonal monsoon strength, it is possible to investigate the relationship between interannual variations of ISO activity and interannual fluctuations of the monsoon. Figure 8 is a scatter diagram of $[\text{OLR}_{\text{EOF}}^2]$ versus OLR_{IM} . The two indices correlate at 0.56, which means that there is an inverse relationship between the strength of the Indian monsoon and the magnitude of summertime ISO activity that explains roughly 25% of the interannual Indian monsoon variance. The inverse relationship is the same sign, although slightly weaker, as that found between wintertime ISO activity and Australian monsoon strength (Hendon et al. 1999). Table 3 lists the correlations between the various monsoon indices and $[\text{OLR}_{\text{EOF}}^2]$. While the correlation of $[\text{OLR}_{\text{EOF}}^2]$ with the two Indian monsoon indices, AIRI and OLR_{IM} , indicates a statistically significant inverse correlation between ISO activity and Indian monsoon strength, the seasonal ISO activity does not appear to be correlated with mean OLR over the Bay of Bengal and hence is not well correlated with total south Asian monsoon mean OLR.

In general, a stronger than normal ISO season corresponds to a weak Indian monsoon. Of the nine seasons in which the $[\text{OLR}_{\text{EOF}}^2]$ index is greater than normal ($>0.5\sigma$), six are deficient Indian monsoon seasons, two are normal Indian monsoon seasons, and only one is an abundant Indian monsoon year (Table 4). Conversely, of the 7 seasons in which the $[\text{OLR}_{\text{EOF}}^2]$ index is below

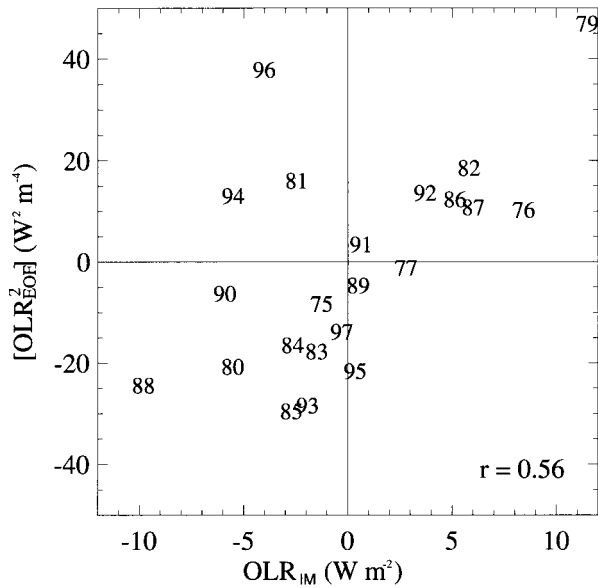


FIG. 8. Scatter diagram of $[OLR^2_{EOF}]$ vs OLR_{IM} . Both indices are plotted as anomalies from their respective 22-yr means. The correlation is 0.56.

normal ($< -0.5\sigma$), four are wet Indian monsoon seasons, three are near normal, while none are abnormally dry.

The inverse relationship between Indian monsoon strength and ISO activity is examined further by compositing the mean OLR_{EOF} wavelet spectra for wet and dry monsoon seasons. The composite wavelet spectrum of the five wettest Indian monsoon seasons (1975, 1980, 1983, 1988, 1990) is shown in Fig. 9 (top panels). The ISO variance is below normal throughout the season although more so at the beginning of the season. There is a slight indication that the period of oscillation is reduced to near 33 days during wet monsoons, but, as noted previously, the flatness of the frequency spectrum when the average variance is low precludes one from making a definitive statement about the oscillation period. Out of the five wet monsoon seasons composited, two are also classified as cool JJAS Niño-3 SST years. A separate composite (not shown), consisting solely of the three wettest monsoon years that are not also cool JJAS Niño-3 SST years, exhibits the same general characteristics as that shown in Fig. 9.

TABLE 3. Correlations between seasonal ISO activity index ($[OLR^2_{EOF}]$) and south Asian monsoon indices over 22 yr (1975–97, excluding 1978). A correlation coefficient greater than ± 0.36 is statistically significant at 95% confidence level.

Monsoon index	JJAS ISO activity	
	$[OLR^2_{EOF}]$	
AIRI	-0.45	
OLR_{SAM}	0.30	
OLR_{IM}	0.56	
OLR_{BB}	0.17	

TABLE 4. Number of strong, normal, and weak Indian monsoon seasons corresponding to high- or low-ISO activity seasons.

	$[OLR^2_{EOF}]$	
	$> 0.5\sigma$	$< -0.5\sigma$
Strong monsoon	1	4
Normal monsoon	2	3
Weak monsoon	6	0

The composite OLR_{EOF} wavelet spectrum of the five driest monsoon seasons (1976, 1979, 1982, 1986, 1987) is shown in Fig. 9 (bottom panels). The variance is above normal at all times and scales. Once again, of the five driest monsoon seasons composited, two are also classified as warm JJAS Niño-3 SST years. The composite wavelet spectrum of the remaining three dry monsoon years (not shown) is largely similar except that the late monsoon season variance is substantially stronger

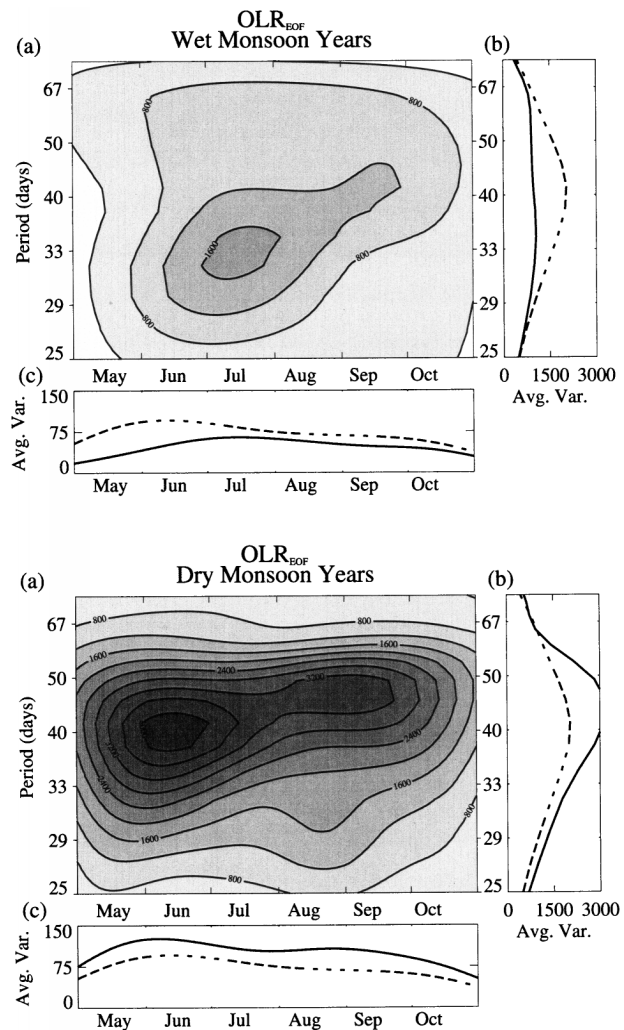


FIG. 9. Same as Fig. 6 but composite of (top) five wettest Indian monsoon years (1975, 1980, 1983, 1988, 1990) and (bottom) five driest Indian monsoon years (1976, 1979, 1982, 1986, 1987).

than the composite values seen in Fig. 9, while the early season variance is closer to normal levels.

c. Relation to interannual SST variability

1) ENSO

Because of the established inverse relationship between ENSO and the south Asian monsoon, it is important to examine the associations between ISO activity and ENSO to assess whether or not, for example, increased ISO activity during a weak Indian monsoon is simply a result of an enhancement of ISO activity induced by warm eastern tropical Pacific Ocean SST anomalies. The simultaneous correlation between JJAS Niño-3 SST and $[OLR_{EOF}^2]$ is only weakly positive at 0.16. This result is consistent with the results of Hendon et al. (1999) who found that wintertime ISO activity is essentially uncorrelated with DJF Niño-3 SST, although they noted that significant reductions in wintertime ISO activity were observed during the two strongest recent ENSO events (1982/83, 1997/98). Of the four warmest JJAS Niño-3 SST years included in this study, two exhibit above-normal $[OLR_{EOF}^2]$ levels (1982, 1987) and two exhibit below-normal $[OLR_{EOF}^2]$ levels (1983, 1997). In contrast, of the coolest four JJAS Niño-3 SST years, three exhibit below-normal $[OLR_{EOF}^2]$ values (1975, 1985, 1988) while one exhibits above-normal $[OLR_{EOF}^2]$ values (1981). This breakdown emphasizes the result that ISO activity is not clearly linked to ENSO phase with above- or below-normal ISO activity nearly equally probable during either warm or cool JJAS Niño-3 SST years.

Composites of the OLR_{EOF} wavelet spectra for the four warmest and four coolest JJAS Niño-3 SST years are shown in Fig. 10. For the warm JJAS Niño-3 SST composite (top panels), the OLR_{EOF} variance tends to be above normal at the beginning of the monsoon season in May–July and below normal for the remainder of the season such that the total summertime variance is near normal. For the cool JJAS Niño-3 SST composite (bottom panels) the early part of the monsoon season is characterized by weaker-than-normal ISO activity while the remainder of the season exhibits near-normal ISO activity. It is important to note that the composites shown in Fig. 10 include only four seasons each; consequently, these results must solely be considered indicative rather than definitive. Nevertheless, the modest positive correlation between mean seasonal ISO activity and ENSO appears due to changes in early monsoon season ISO activity associated with the state of ENSO. Correlations between JJAS Niño-3 SST and ISO activity are 0.38 for the first two months of the monsoon season and only -0.03 for the latter two months of the season.

The mean frequency spectra of the OLR_{EOF} wavelet spectra composites for warm and cool JJAS Niño-3 SST are shown in Fig. 10b. No distinguishable shift in ISO period can be discerned during either ENSO phase. The lack of an observed period shift associated with the

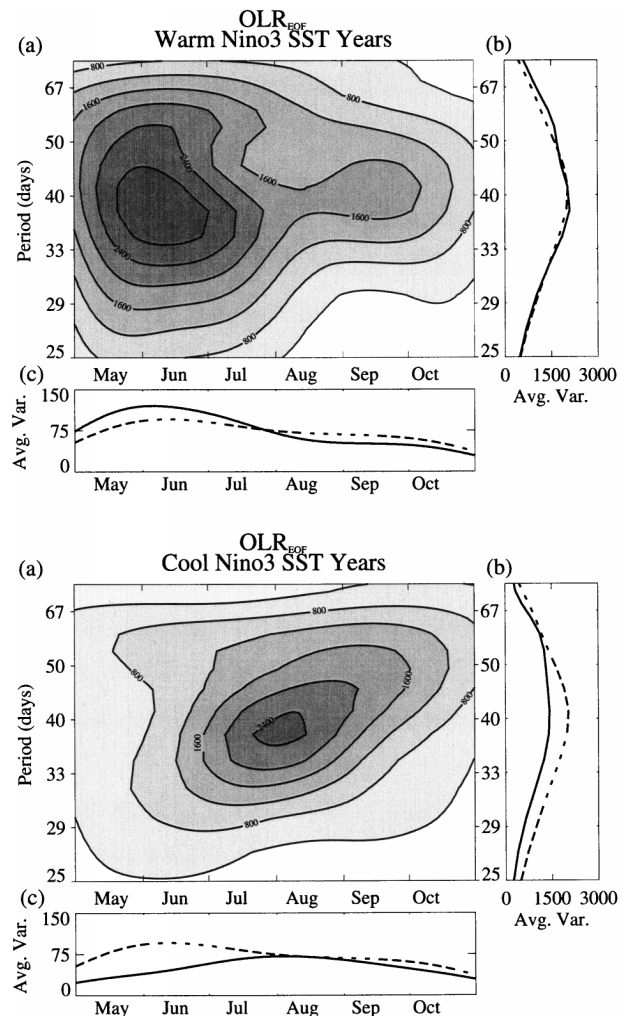


FIG. 10. Same as Fig. 6 but composite of (top) four warmest JJAS Niño-3 SST years (1982, 1983, 1987, 1997) and (bottom) four coolest JJAS Niño-3 SST years (1975, 1981, 1985, 1988). Dashed lines show mean variance from all-years composite.

phase of ENSO runs counter to the model results of Krishnan and Kasture (1996), in which they found that warm ENSO years are characterized by slower oscillations. However, Krishnan and Kasture also found that warm ENSO seasons exhibit more regular ISO behavior, a result that is weakly supported by the analysis completed here.

To summarize the preceding analysis, the phase of ENSO during northern summer does not appear to strongly impact the amplitude or location of seasonally averaged summertime ISO activity. However, at the beginning of the monsoon season ISO activity may be influenced by the phase of ENSO with moderately enhanced ISO activity observed during the warm ENSO phase and vice versa, a relationship that could be a factor in terms of predicting the monsoon onset. Confidence in the robustness of the subtle intraseasonal changes in ISO activity during warm or cool ENSO years is low

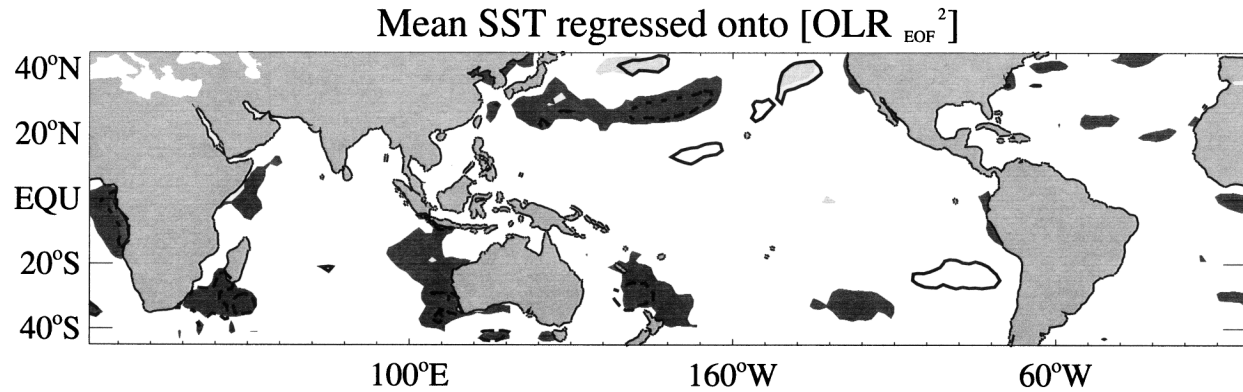


FIG. 11. Regression of Jun–Sep anomalous SST onto $[\text{OLR}_{\text{EOF}}^2]$. Contour intervals are every 0.25°C beginning at $\pm 0.125^\circ\text{C}$. Black lines denote where correlation coefficients are significant at 95% level based on 22 dof (± 0.36).

because of the small number of warm and cool ENSO seasons included in this study, but it may warrant further examination particularly because of the importance of the timing of the monsoon onset for agriculture and water management in south Asia.

2) OTHER SST VARIABILITY

To explore the possible role of SST anomalies other than those associated with ENSO the global summertime mean SST is regressed onto the $[\text{OLR}_{\text{EOF}}^2]$ index (Fig. 11). The regression map shows that there is virtually no coincident relationship between any tropical SST anomalies and summertime ISO activity. It is also possible that ISO activity is impacted by lead SST anomalies. We completed similar regressions to those shown in Fig. 11 for leads up to one year and did not find any notable lag–lead relationships between SST anomalies and summertime ISO activity. Hence, the importance of SST boundary forcing on the level of ISO activity seems to be minimal although it remains possible that small interannual changes in SST generate large year-to-year changes in ISO activity in a nonlinear manner.

3) ISO ACTIVITY, INDIAN MONSOON, AND ENSO

The results discussed above suggest that both the level of ISO activity and the state of ENSO bear some relationship to Indian monsoon strength and furthermore that ISO activity is not highly dependent on the state of ENSO. Figures 12a and 12b display the regressions of summertime mean OLR onto $[\text{OLR}_{\text{EOF}}^2]$ and JJAS Niño-3 SST, respectively. OLR that is linearly dependent on JJAS Niño-3 SST is removed prior to forming the regression in Fig. 12a. In a similar manner, OLR that is linearly dependent on $[\text{OLR}_{\text{EOF}}^2]$ is removed prior to forming the regression of mean OLR onto JJAS Niño-3 SST shown in Fig. 12b. The anomaly patterns in Fig. 12b resemble the classic large-scale anomaly patterns associated with ENSO including enhanced convection

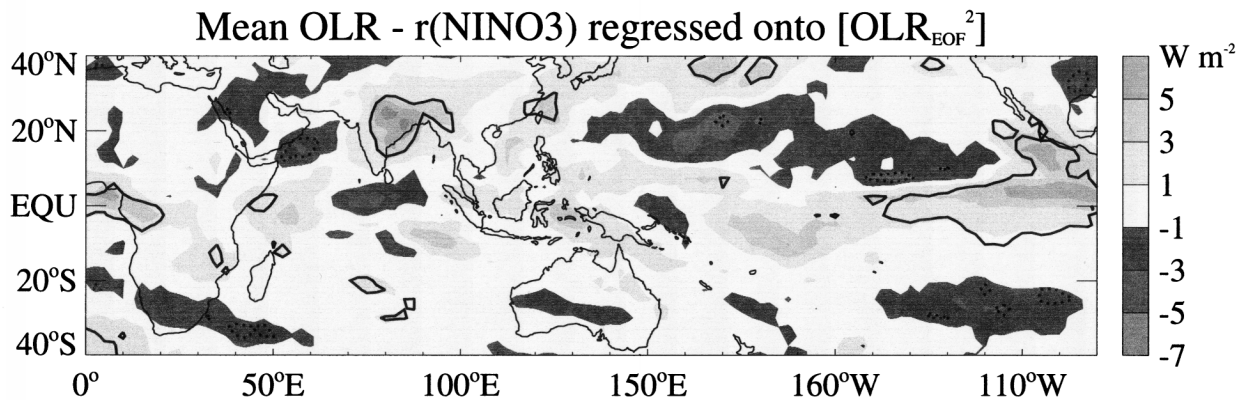
over the eastern Pacific Ocean and reduced convection over Indonesia, equatorial Africa, and peninsular India (e.g., Kiladis and Diaz 1989). Meanwhile, as anticipated by the inverse relationship between OLR_{IM} and $[\text{OLR}_{\text{EOF}}^2]$, independent of ENSO, strong ISO activity corresponds to reduced convection over most of India and Bangladesh, but is relatively unassociated with convection over the Bay of Bengal (Fig. 12a). This figure emphasizes the point that the relationship between Indian monsoon and ISO activity is of equal or greater magnitude than that with ENSO during the period 1975–97. Regression maps created without removing OLR that is linearly dependent on $[\text{OLR}_{\text{EOF}}^2]$ and ENSO are qualitatively similar due to low mutual correlation between $[\text{OLR}_{\text{EOF}}^2]$ and JJAS Niño-3 SST.

6. Discussion and conclusions

An objective index that captures the interannual variability of summertime ISO activity over south Asia is developed. The index is based on extraction of the summertime ISO signal in the first two inseparable EOF modes of intraseasonally filtered OLR. Summertime ISO activity is inversely correlated, at approximately -0.45 to -0.56 , with Indian monsoon strength (see Table 3). The inverse correlation with Bay of Bengal convection is much weaker (-0.17), thereby reducing the correlation with the total south Asian monsoon convection (-0.30). The reason why ISO activity is inversely correlated with convection over land but not over the ocean is unclear although it may have some bearing on the somewhat independent interannual variability of convection in these two regions of the south Asian monsoon.

Singh et al. (1992), who examined ISO activity by analyzing 80 years of daily station rainfall data, conclude that there is no relationship between ISO activity and seasonal mean Indian monsoon rainfall, a result that contradicts the findings of this study. It is possible that the apparent contradiction between our results and those of Singh et al. may be due to decadal-timescale changes

(a)



(b)

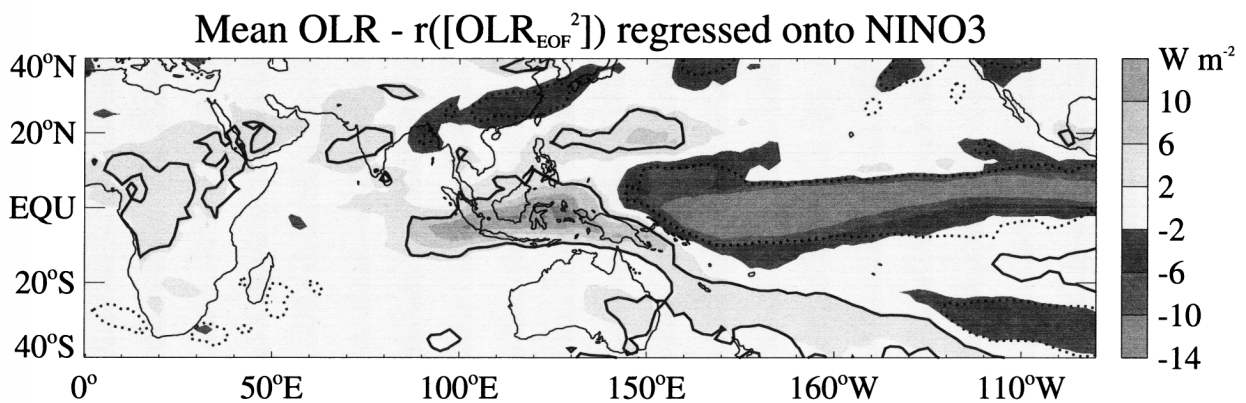


FIG. 12. Regression of Jun–Sep mean OLR onto (a) $[\text{OLR}_{\text{EOF}}^2]$ and (b) Niño-3 SST. Prior to forming the regressions, OLR that is (a) linearly dependent on Niño-3 SST and (b) linearly dependent on $[\text{OLR}_{\text{EOF}}^2]$ is removed. OLR anomalies are shown for a 1.5σ anomaly of $[\text{OLR}_{\text{EOF}}^2]$ and Niño-3 SST, respectively. Black lines outline regions where correlation coefficients are significant at the 95% level based on 22 dof (± 0.36).

in ISO activity. Slingo et al. (1999) found evidence that global ISO activity was markedly reduced in the period 1958–76 as compared with recent years (although it remains unclear whether their result is an artifact of the NCEP–NCAR reanalysis). A significant reduction in the level of global ISO activity would contribute to lower correlations between ISO activity and Indian monsoon rainfall during those periods.

The total explained variance of the summer mean rainfall over India by interannual variations of ISO activity is modest (25%). Nevertheless, the variance explained is of comparable or greater magnitude to that explained by ENSO (at least during the period 1975–97), which is generally considered an important factor for Indian monsoon variability. Since the correlations between ISO activity and JJAS Niño-3 SST, or any global SST anomalies for that matter, are small, the relationship between ISO activity and Indian monsoon strength is largely independent of the relationship between ENSO phase and Indian monsoon strength.

In the case of the ENSO–monsoon relationship, the

separation between cause and effect is not clear; that is, ENSO may drive variations in the monsoon or the monsoon may be a factor in the evolution of ENSO (Webster and Yang 1992). Similarly, it is difficult to separate whether changes in ISO activity force changes in monsoon strength or vice versa. The lack of any clear relationship between ISO activity and global SST anomalies implies that interannual variability of ISO activity is either internally generated or is forced by land surface boundary conditions. Hendon et al. (1999) argue that a weak Australian monsoon could enhance wintertime ISO activity by shifting the mean convection distribution closer to the equator, which presumably is a more favorable condition for ISO formation (e.g., Wang and Li 1994; Salby et al. 1994). In that scenario, variations in monsoon strength force variations in ISO activity. This could occur during summer with a weak continental south Asian monsoon permitting stronger ISO activity. However, there is a problem with this theory. The deepest off-equatorial monsoon convection lies over the Bay of Bengal where interannual changes in mean convec-

tion are relatively unresponsive to interannual shifts in ISO activity (correlation of -0.18). The low correlation says that some seasons characterized by strong off-equatorial ISO activity are also characterized by deep off-equatorial convection that, according to the theory of Hendon et al., would inhibit ISO activity. The lack of a clear boundary condition that is associated with changes in ISO activity suggests that the variations may be internally and chaotically generated or are due to an as yet unidentified boundary condition. Since the ISO is at least quasiperiodic, it is possible that ISO activity exhibits some persistence across seasons; that is, years exhibiting strong wintertime and springtime ISO activity may be followed by strong summertime ISO activity. Correlations between wintertime and springtime ISO activity indices, derived in a similar manner to that described by Hendon et al. (1999), and our summertime ISO activity index are small, which indicates that there is not a great degree of persistence in ISO activity from season to season.

Whether interannual monsoon variability forces interannual fluctuations of ISO activity or vice versa, the relatively strong inverse correlation between the two phenomena has implications for forecasting. A dynamic model that cannot generate an accurate representation of the ISO will likely have a difficult time accurately predicting Indian monsoon strength, particularly during weak monsoons when ISO activity is often strong.

An inconclusive result of this study that is worthy of further attention is the seasonal evolution of summertime ISO activity. According to Fig. 6, ISO activity is strongest at the beginning of summer before it tails off over the course of the monsoon season. Additionally, there is limited evidence that the phase of ENSO affects ISO activity in June and July but not during the rest of the season. Furthermore, dry monsoon seasons that are not also warm ENSO seasons tend to exhibit substantially greater than normal ISO activity during the latter half of the monsoon season. The causes and implications of such intraseasonal variations in ISO activity are not clear and warrant further investigation.

Acknowledgments. We thank George Kiladis for useful comments on an earlier draft of this manuscript. This research was supported by NSF Grant ATM-9526030. OLR, NCEP-NCAR reanalysis, and Reynolds SST data were provided by the NOAA-CIRES Climate Diagnostic Center, Boulder, Colorado, from their Web site at <http://www.cdc.noaa.gov/>.

REFERENCES

- Brankovic, C., and T. N. Palmer, 2000: Seasonal skill and predictability of ECMWF PROVOST ensembles. *Quart. J. Roy. Meteor. Soc.*, **126**, 2035–2068.
- Camberlin, P., 1997: Rainfall anomalies in the source region of the Nile and their connection with the Indian summer monsoon. *J. Climate*, **10**, 1380–1392.
- Chowdhury, A., R. K. Mukhopadhyay, and K. C. Sinha Ray, 1988: Low frequency oscillations in summer monsoon rainfall over India. *Mausam*, **39**, 375–382.
- Clark, C. O., J. E. Cole, and P. J. Webster, 2000: Indian Ocean SST and Indian summer rainfall: Predictive relationships and their decadal variability. *J. Climate*, **13**, 2503–2519.
- Elliot, W. P., and J. K. Angell, 1988: Evidence for changes in Southern Oscillation relationships during the last 100 years. *J. Climate*, **1**, 729–737.
- Ferranti, L., J. M. Slingo, T. N. Palmer, and B. J. Hoskins, 1997: Relations between interannual and intraseasonal monsoon variability as diagnosed from AMIP integrations. *Quart. J. Roy. Meteor. Soc.*, **123**, 1323–1357.
- Fink, A., and P. Speth, 1997: Some potential forcing mechanisms of the year-to-year variability of the tropical convection and its intraseasonal (25–70-day) variability. *Int. J. Climatol.*, **17**, 1513–1534.
- Gadgil, S., and G. Asha, 1992: Intraseasonal variations of the Indian summer monsoon. Part I: Observational aspects. *J. Meteor. Soc. Japan*, **70**, 517–527.
- Goswami, B. N., V. Krishnamurthy, and H. Annamalai, 1999: A broad-scale circulation index for the interannual variability of the Indian summer monsoon. *Quart. J. Roy. Meteor. Soc.*, **125**, 611–633.
- Gutzler, D. S., 1991: Interannual fluctuations of intraseasonal variance of near-equatorial zonal winds. *J. Geophys. Res.*, **96**, 3173–3185.
- Harzallah, R., and R. Sadourny, 1997: Observed lead-lag relationships between Indian summer monsoon and some meteorological variables. *Climate Dyn.*, **13**, 635–648.
- Hendon, H. H., and M. L. Salby, 1994: The life cycle of the Madden-Julian oscillation. *J. Atmos. Sci.*, **51**, 2225–2237.
- , C. Zhang, and J. D. Glick, 1999: Interannual variation of the Madden-Julian oscillation during austral summer. *J. Climate*, **12**, 2538–2550.
- Ju, J., and J. Slingo, 1995: The Asian summer monsoon and ENSO. *Quart. J. Roy. Meteor. Soc.*, **121**, 1133–1168.
- Julian, P. R., and R. A. Madden, 1981: Comments on a paper by T. Yasunari: A quasistationary appearance of 30 to 40 day period in the cloudiness fluctuations during the summer monsoon over India. *J. Meteor. Soc. Japan*, **59**, 435–437.
- Kiladis, G. N., and H. F. Diaz, 1989: Global climatic anomalies associated with extremes in the Southern Oscillation. *J. Climate*, **2**, 1069–1090.
- Krishna Kumar, K., M. K. Soman, and K. Rupa Kumar, 1995: Seasonal forecasting of Indian summer monsoon rainfall. *Weather*, **50**, 449–467.
- Krishnan, R., and S. V. Kasture, 1996: Modulation of low frequency intraseasonal oscillations of northern summer monsoon by El Niño and Southern Oscillation (ENSO). *Meteor. Atmos. Phys.*, **60**, 237–257.
- Kumar, K. K., B. Rajagopalan, and M. A. Cane, 1999: On the weakening relationship between the Indian monsoon and ENSO. *Science*, **284**, 2156–2159.
- Lau, K.-M., and P. H. Chan, 1986: Aspects of the 40–50 day oscillation during the northern summer as inferred from outgoing longwave radiation. *Mon. Wea. Rev.*, **114**, 1354–1367.
- Liebmann, B., and C. A. Smith, 1996: Description of a complete (interpolated) outgoing longwave radiation dataset. *Bull. Amer. Meteor. Soc.*, **77**, 1275–1277.
- Madden, R. A., 1986: Seasonal variations of the 40–50 day oscillation in the Tropics. *J. Atmos. Sci.*, **43**, 3138–3158.
- Meehl, G. A., 1987: The annual cycle and interannual variability in the tropical Pacific and Indian Ocean region. *Mon. Wea. Rev.*, **115**, 27–50.
- , 1997: The South Asian monsoon and the tropospheric biennial oscillation. *J. Climate*, **10**, 1921–1943.
- Mehta, A. V., and T. N. Krishnamurti, 1988: Interannual variability of the 30–50 day wave motions. *J. Meteor. Soc. Japan*, **66**, 535–548.
- Mooley, D. A., and B. Parthasarathy, 1984: Fluctuations in all-India

- summer monsoon rainfall during 1871–1978. *Climatic Change*, **6**, 287–301.
- North, G. R., T. L. Bell, R. F. Chahalan, and F. J. Moeng, 1982: Sampling errors in the estimation of empirical orthogonal functions. *Mon. Wea. Rev.*, **110**, 699–706.
- Parthasarathy, B., R. R. Kumar, and D. R. Kothawale, 1992: Indian summer monsoon rainfall indices, 1871–1990. *Meteor. Mag.*, **121**, 174–186.
- , A. A. Munot, and D. R. Kothawale, 1994: All India monthly and seasonal rainfall series: 1871–1993. *Theor. Appl. Climatol.*, **49**, 217–224.
- Rao, K. G., and B. N. Goswami, 1988: Interannual variations of sea surface temperature over the Arabian Sea and the Indian monsoon: A new perspective. *Mon. Wea. Rev.*, **116**, 558–568.
- Reynolds, R. W., and T. M. Smith, 1994: Improved global sea surface temperature analyses using optimum interpolation. *J. Climate*, **7**, 929–948.
- Salby, M. L., R. R. Garcia, and H. H. Hendon, 1994: Planetary-scale circulations in the presence of climatological wave-induced heating. *J. Atmos. Sci.*, **51**, 2344–2366.
- Sikka, D. R., and S. Gadgil, 1980: On the maximum cloud zone and the ITCZ over Indian longitudes during the southwest monsoon. *Mon. Wea. Rev.*, **108**, 1840–1853.
- Singh, S. V., R. H. Kripalani, and D. R. Sikka, 1992: Interannual variability of the Madden–Julian oscillations in Indian summer monsoon rainfall. *J. Climate*, **5**, 973–978.
- Slingo, J. M., D. P. Rowell, K. R. Sperber, and F. Nortley, 1999: On the predictability of the interannual behaviour of the Madden–Julian oscillation and its relationship with El Niño. *Quart. J. Roy. Meteor. Soc.*, **125**, 583–609.
- Smith, T. M., R. W. Reynolds, R. E. Livezey, and D. C. Stokes, 1996: Reconstruction of historical sea surface temperatures using empirical orthogonal functions. *J. Climate*, **9**, 1403–1420.
- Sperber, K. R., J. M. Slingo, and H. Annamalai, 2000: Predictability and the relationship between subseasonal and interannual variability during the Asian summer monsoon. *Quart. J. Roy. Meteor. Soc.*, **126**, 2545–2574.
- Torrence, C., and G. Compo, 1998: A practical guide to wavelet analysis. *Bull. Amer. Meteor. Soc.*, **79**, 61–78.
- , and P. J. Webster, 1998: The annual cycle of persistence in the El Niño/Southern Oscillation. *Quart. J. Roy. Meteor. Soc.*, **124**, 1985–2004.
- , and —, 1999: Interdecadal changes in the ENSO–Monsoon system. *J. Climate*, **12**, 2679–2690.
- Vernekar, A. D., V. Thapliyal, R. H. Kripalani, S. V. Singh, and B. Kirtman, 1993: Global structure of the Madden–Julian oscillations during two recent contrasting summer monsoon seasons over India. *Meteor. Atmos. Phys.*, **52**, 37–47.
- , J. Zhou, and J. Shukla, 1995: The effect of Eurasian snow cover on the Indian monsoon. *J. Climate*, **8**, 248–266.
- Wainer, I., and P. J. Webster, 1996: Monsoon/El Niño–Southern Oscillation relationships in a simple couple ocean–atmosphere model. *J. Geophys. Res.*, **101**, 25 599–25 614.
- Wang, B., and H. Rui, 1990: Synoptic climatology of transient tropical intraseasonal convection anomalies: 1975–1985. *Meteor. Atmos. Phys.*, **44**, 43–61.
- , and T. Li, 1994: Convective interaction with boundary-layer dynamics in the development of a tropical intraseasonal system. *J. Atmos. Sci.*, **51**, 1386–1400.
- , and Z. Fan, 1999: Choice of South Asian summer monsoon indices. *Bull. Amer. Meteor. Soc.*, **80**, 629–638.
- Webster, P. J., 1995: The annual cycle and the predictability of the tropical couple ocean–atmosphere system. *Meteor. Atmos. Phys.*, **56**, 33–55.
- , and S. Yang, 1992: Monsoon and ENSO: Selectively interactive systems. *Quart. J. Roy. Meteor. Soc.*, **118**, 877–926.
- , and T. N. Palmer, 1997: The past and future of El Niño. *Nature*, **390**, 562–564.
- , V. O. Magaña, T. N. Palmer, J. Shukla, R. A. Tomas, M. Yanai, and T. Yasunari, 1998: Monsoons: Processes, predictability, and the prospects for prediction. *J. Geophys. Res.*, **103**, 14 451–14 510.
- Xie, P., and P. A. Arkin, 1996: Analyses of global monthly precipitation using gauge observations, satellite estimates and numerical model predictions. *J. Climate*, **9**, 840–858.
- Yang, S., 1996: ENSO–snow–monsoon associations and seasonal-to-interannual predictions. *Int. J. Climatol.*, **16**, 125–134.
- Yasunari, T., 1979: Cloudiness fluctuations associated with the Northern hemisphere summer monsoon. *J. Meteor. Soc. Japan*, **57**, 227–242.
- , 1980: A quasi-stationary appearance of 30 to 40 day period in the cloudiness fluctuations during the summer monsoon over India. *J. Meteor. Soc. Japan*, **58**, 225–229.
- , 1990: Impact of Indian monsoon on the coupled atmosphere/ocean system in the tropical Pacific. *Meteor. Atmos. Phys.*, **44**, 29–41.